

# Orbital evolution of meteoroids from short period comets

G. Cremonese<sup>1</sup>, M. Fulle<sup>2</sup>, F. Marzari<sup>3</sup>, and V. Vanzani<sup>3</sup>

<sup>1</sup> Osservatorio Astronomico, vic. Osservatorio 5, I-35122 Padova, Italy

<sup>2</sup> Osservatorio Astronomico, via Tiepolo, I-34 Trieste, Italy

<sup>3</sup> Dipartimento di Fisica, Università di Padova, Via Marzolo 8, I-35131 Padova, Italy

Received 17 August 1995 / Accepted 9 August 1996

**Abstract.** We perform an accurate modelling of orbital evolution of dust grains taking into account both the ejection parameters derived from the analysis of the dust tail of each considered parent comet (Fulle 1989), and the integration of the Newton equations in the context of a nine-body problem (Sun, seven major planets and the dust particle) plus solar radiation and wind forces. Among Short Period Comets (SPC) we have selected P/Schwassmann–Wachmann 1 (P/SW1) and P/Griegg–Skjellerup (P/GS), which represent two significantly different objects from a dynamical point of view. Dust from P/SW1 is dominated by Jupiter perturbations: after  $2 \cdot 10^4$  years, about 7% of the grains are ejected in hyperbolic orbits, 80% of the grains have the perihelion out of 4 AU from the Sun, and only 1% of them reaches the Sun distance of 1 AU, thus contributing to the inner zodiacal cloud. Dust from P/GS is dominated by the P–R drag, although large grains, due to their longer collapse lifetime, are sensitive to Jupiter perturbations. Therefore the Tisserand criterion represents a useful tool both to estimate the orbital evolution of grains larger than  $100 \mu\text{m}$  (i.e. the most likely candidates to replenish the zodiacal dust cloud, Grün et al. 1985), and in distinguishing the parent sources of meteoroids collected with near Earth space experiments able to measure the impact velocity vectors. Jupiter perturbations oppose to the P–R drag forces and reduce significantly the contribution of SPC to the inner zodiacal dust: the simple sum of the dust mass contribution from each SPC may be an overestimate of their actual supply.

**Key words:** celestial mechanics – interplanetary medium – comets, P/Griegg–Skjellerup; comet: P/Schwassmann–Wachmann 1 – meteors, meteoroids

## 1. Introduction

Short-period comets (hereafter SPC) are one of the most likely sources of interplanetary dust. To estimate their actual contribution to the dust mass in the zodiacal cloud, we have to know the

*Send offprint requests to:* G. Cremonese

dust production rate and the fraction of grains injected in bound orbits. The average dust production rate of SPC was assumed to be about  $10^5 r^{-2} \text{ g s}^{-1}$ , where  $r$  is the Sun–comet distance in AU (Mukai 1989), but it can vary significantly among SPC. The orbital evolution of cometary dust particles depends on the starting orbital parameters related to the ejection velocity, on solar gravitational, radiation and corpuscular forces and on gravitational perturbations by planets. In this paper we discuss the orbital evolution of the dust emitted by two short period comets characterized by very different orbits, namely P/Schwassmann–Wachmann 1 (P/SW1) and P/Griegg–Skjellerup (P/GS). P/SW1 is a trans-Jupiter object, so that all the dust released from this comets is heavily perturbed by Jupiter during its orbital collapse towards the inner Solar System. On the other hand, P/GS aphelium does not reach the Jupiter Sun distance, so that the orbital evolution of the dust released from this comet should be more sensitive to radiation drag effects than P/SW1 meteoroids.

Both comets have been analyzed by means of the inverse numerical model of comet dust tails and outer comae developed by Fulle (1989), which gives information on the dust size (diameter) distribution, production rate, emission anisotropy and velocity. P/GS has been the second target of the GIOTTO mission and there have been efforts to get ground-based observations at the same time of the probe fly-by. In this way it was possible, by applying the quoted tail model, to compare ground-based results with in-situ dust measurements (McDonnell et al. 1992), performing a check of the model and giving more reliability to the parameters of the dust particles. The main output of both approaches was that P/GS, as P/Halley, produces dust with its mass lying all in the largest grains, with a perihelion mass loss rate of  $200 \text{ kg s}^{-1}$  and a dust ejection velocity of  $15 \text{ m s}^{-1}$  for grains with a diameter of 0.15 mm (Fulle, et al., 1993), so that this minor short-period comet too might be a significant zodiacal dust source.

The P/SW1 tail modeling was devoted to estimate the possible meteoroid supply from trans-Jupiter sources (Fulle, 1992). A surprising tail model output was the high P/SW1 dust mass loss rate, larger than  $300 \text{ kg s}^{-1}$ , ten times larger than the value suggested by early coma observations (Jewitt 1990), interpreted assuming unrealistic dust velocities. According to the

calculations performed by Fulle (1992) the P/SW1 apparently provides  $\sim 6\%$  of the mass required to balance the losses of the interplanetary dust cloud. Furthermore direct radio observations have provided evidence of a CO mass loss rate close to  $2000 \text{ kg s}^{-1}$  (Senay & Jewitt 1994), so that the inverse tail model output becomes a realistic lower limit of actual dust mass loss rate. Since the meteoroid supply from trans-Jupiter sources is ruled by Jupiter perturbations on the dust orbits, an original result of this paper will be the estimate of the percentage of meteoroids which enter the Jupiter orbit. Taking into account the results on the emission anisotropy and velocity provided by inverse tail model, it is possible to follow the orbital evolution of dust grains leaving the parent comet with a relative velocity different from zero. The trajectories of the particles are then integrated in the context of a nine-body problem (Sun, seven major planets and the dust particle) with the solar radiation and wind forces accounted for.

## 2. Model for dust ejection

Cometary dust is released from the nucleus surface by ice sublimation with negligible initial velocity. Then dust is dragged out by the expanding gas in the coma, and at about ten nuclear radii the grain reaches its terminal velocity (Crifo 1991). For the largest particles, the deceleration due to nucleus gravity must be taken into account (Wallis 1982). Detailed dust-gas interaction models (Gombosi 1986, Crifo 1987) allow to obtain the time and size dependent dust ejection velocity, but they require precise data on the nucleus size, on the gas loss rate, and on the dust size distribution. These quantities are affected by large uncertainties, and are unavailable for the comets we consider. Moreover, no in-situ experiment has test such models. Ground-based observations require multi-parametric models to extract information on the dust velocity, and provide results which can be compared with the outputs of dust-gas drag theory.

All models describing dust comae and tails must take into account the time and size dependence of the dust ejection velocity as free parameters. In the majority of these models, the dust velocity is an input parameter, and the sensitivity of the model results on it was never tested. It follows that the successful fits of these models with observations never provided any information on the reliability of the adopted dust ejection velocity. To our knowledge, two models only consider the dust velocity as an output parameter, thus providing a significant test of dust-gas drag theory: dust tail models (Finson & Probst 1968, Kimura & Liu 1977, Richter & Keller 1987, Fulle 1987, Fulle 1989) and neck-line models (Fulle & Sedmak 1988, Cremonese & Fulle 1989). Tail models provide the time dependence of the dust velocity, whereas its size dependence must be treated as an input parameter. Then it is necessary to test the sensitivity of the model output on this input parameter. Neck-line models provide directly the size dependence of the dust velocity and the velocity value at a fixed time.

For the large sizes typical of meteoroids, dust-gas drag theory provides a dust velocity size dependence which can well be approximated by a power law with index  $u = \frac{\partial \log v}{\partial \log s}$  of the

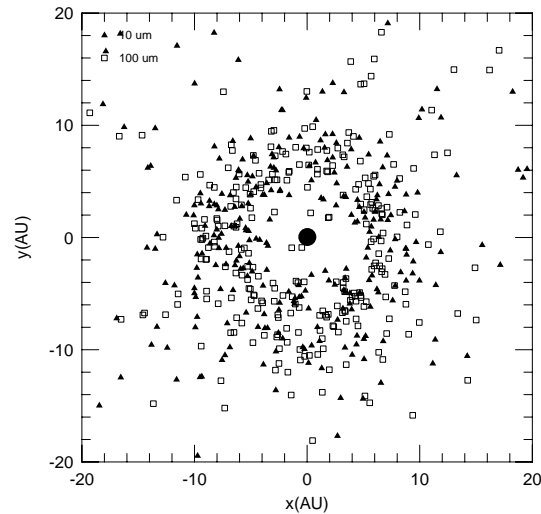


**Fig. 1.** Spatial distribution of dust grains emitted by comet P/SW1 at the 1989 perihelion passage. The orbits of the particles have been integrated for  $5 \cdot 10^3$  years after the ejection. Filled triangles represent  $10 \mu\text{m}$  size (diameter) grains, empty squares  $100 \mu\text{m}$  size grains

dust diameter  $s$ . All models (Crifo 1991) provide  $u = -0.5$  for  $s > 10 \mu\text{m}$ . However, the results of neck-line models provide  $-0.25 < u < -0.15$ . Exotic phenomena as dust fragmentation or gas evaporation seem to be possible explanations of  $u > -0.5$ , but detailed and realistic models of so complex dust behaviours are not available (Crifo 1991). A prudent conclusion is that all dust coma and tail models should test the sensitivity of their results on all power indices  $-0.5 < u < -0.15$ , but this approach was followed in the applications of the inverse Monte-Carlo dust tail model only (Fulle 1989). Since the aim of this paper is to verify the sensitivity of meteoroid orbital evolution on its ejection velocity, we are forced to take into account the results provided by the quoted inverse tail model.

The kernel of the inverse tail model is an automatic least square fit of the observed tail images with the model tail images. The free parametric function which allows to minimize the residual of such least square fit is the product of the dust loss rate times the time-dependent size distribution, which are the automatic linear outputs of the model. However, the tail model images too (which are built-up by means of a Monte-Carlo procedure considering keplerian dust dynamics) depend on other free parameters, in particular on the dust ejection velocity. Changes of this non-linear free parameter allow to optimize the data fit and the stability of the linear output. Therefore, inverse Monte-Carlo tail models provide self-consistent estimates of all physical quantities describing a cometary dust environment which do not depend on dust-gas drag models. The performed tests showed a low sensitivity of the model outputs on the power index  $u$  and on the dust ejection anisotropy. Computational details of the inverse model can be found in Fulle et al. (1992).

Inverse tail models can provide information on the dust velocity in limited time and size ranges, because the input images

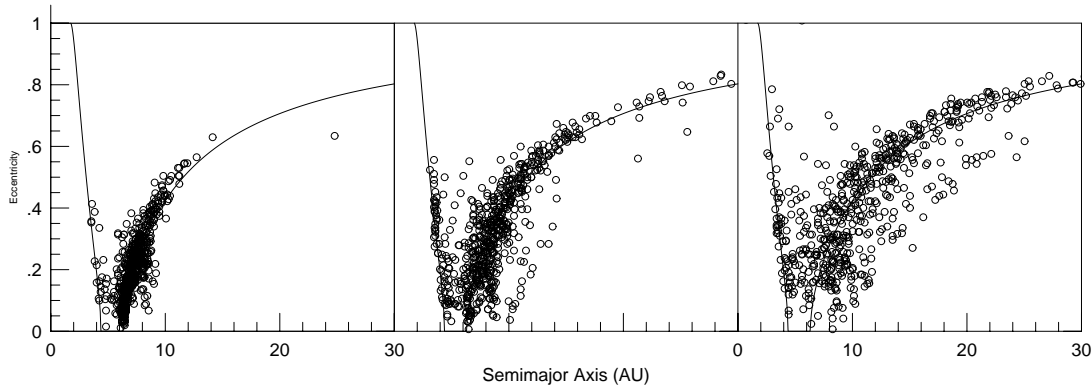


**Fig. 2a.** Orbital distribution of grains in the  $a$ - $e$  plane compared with the Tisserand invariant curve, at different evolutionary times ( $1 \cdot 10^3$ ,  $5 \cdot 10^3$ , and  $2 \cdot 10^4$  years), for P/SW1.

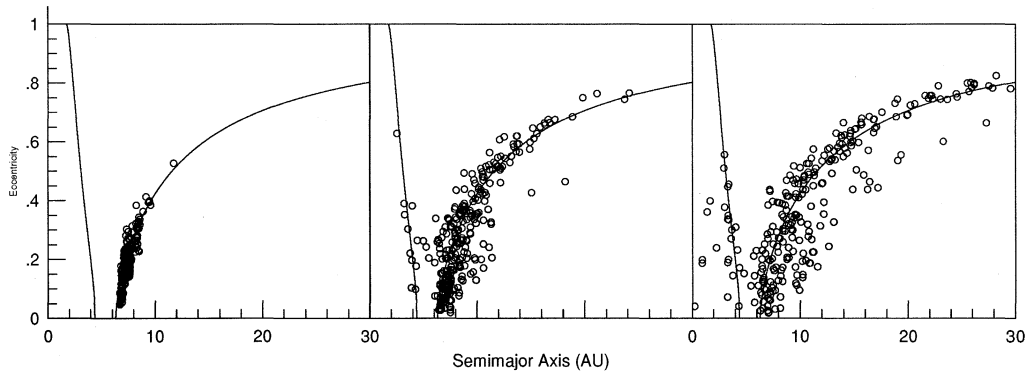


**Fig. 2b.** The same as in Fig. 2a, but including in the drag term the non-radial component of the wind pressure.

have limited size and spatial resolution. We will test the sensitivity of meteoroid orbit evolution on the dust size and ejection anisotropy at a fixed ejection time. Due to the inverse tail model limitations, we will analyse such sensitivity on a dust diameter change of a factor 10 only: from about  $10 \mu\text{m}$  to  $100 \mu\text{m}$  for P/SW1, and from about  $20 \mu\text{m}$  to  $200 \mu\text{m}$  for P/GS. The analysis of the sensitivity of meteoroid orbit evolution on the dust production during long times will be possible for P/SW1 only, because the ground-based observation of P/GS allowed to extract its dust environment during two weeks only around perihelion. For P/SW1, the published results (Fulle 1992) cover about one year before perihelion. We have integrated them with unpublished results obtained from the analysis of P/SW1 steady dust coma images taken in 1993 (Jockers, private communication), in order to extend the time interval to about three years after perihelion. The dust ejection velocity provided by inverse tail model is related to the comet nucleus. Trivial vectorial geometry was applied to compute the starting orbit of each sample dust particle, i.e. the input of orbit evolution codes.

### 3. Numerical integration of dust orbits

The trajectories of the dust particles emitted by the comet are integrated in the context of a nine-body problem (Sun, seven planets – except Mercury and Pluto – and the particle) with

two additional drag terms due to the solar radiation and solar wind forces. These non-gravitational terms in the dust-grain equation of motion, presented in detail in Marzari and Vanzani (1994a, 1994b), include the transverse contribution of the wind pressure arising from the deviation of the wind flow from the radial direction as in Mukai and Yamamoto (1982). The orbits of grains were integrated by RA15 (Everhart, 1985). The choice for this integration method was motivated by the large number of close approaches with Jupiter which require high-precision modelling of fast changes of the planet gravity attraction on the grain. This is undertaken in RA15 by using a variable stepsize.

To express conveniently the non-gravitational terms, we have to assume an appropriate composition for the material of cometary grains. From the data taken by Vega missions on individual grain composition, it turns out that 30% were CHON, 35% were a mixture of CHON and silicates (Mg, Si and Fe) and 35% contained no appreciable content of low atomic number elements except oxygen (Brownlee & Kissel, 1990). A quite strong effect observed by Giotto approaching the nucleus was a decrease in the relative abundance of the C-H-O composition particles with increasing distance from the nucleus. It has been suggested that this could be the result of the sublimation of an intermediate volatility compound such as formaldehyde or formaldehyde polymer. We assume a fluffy structure for the

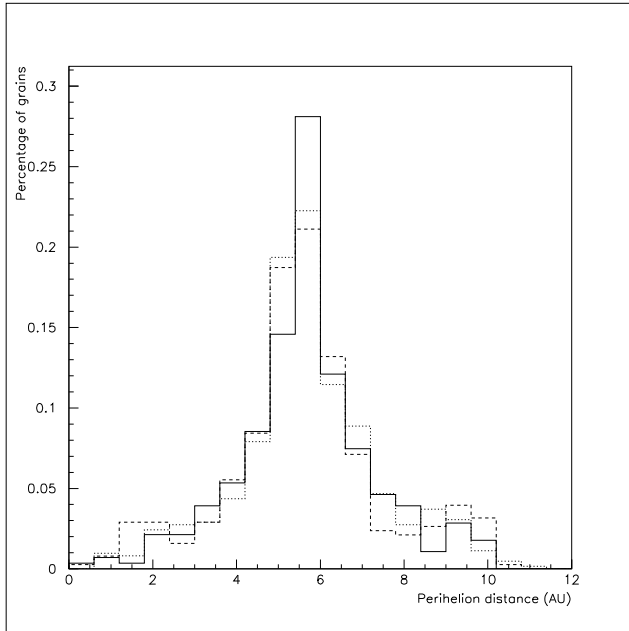


**Fig. 3.** Perihelia distribution at  $t=2 \cdot 10^4$  years for three different sets of dust particles emitted by P/SW1 with different ejection geometry and orbital configurations: isotropical ejection (continuous line), conical ejection (dotted line), multiple ejection (dashed line).

grains with a reference value of bulk density  $\rho = 1 \text{ g cm}^{-3}$ . Sublimation of the water–ice fraction should occur just after the ejection from the cometary nucleus. Further mass loss during the subsequent dynamical evolution is not taken into account. For this material the radiation pressure coefficient averaged over the solar spectrum,  $Q_{pr}$ , is estimated to be about 1. This follows assuming that the dust particles are spherical adopting then the Mie theory. Even if different values of  $\rho$  and  $Q_{pr}$  could be selected, the same value of  $\beta$  can be obtained simply changing the dust particle size.

For the non–gravitational terms we used standard expressions, as in Jackson and Zook (1992), with the ratio of solar wind drag to Poynting–Robertson drag assumed to be 0.3, as by Jackson and Zook. We performed also additional simulations including, as in Marzari and Vanzani (1994a, 1994b), the non–radial component of the wind pressure introduced by Mukai and Yamamoto (1982) to account for a non–radial flow of the solar wind, as resulting on a theoretical basis. However, as pointed out by Gustafson (1994), observational results on this non–radial flux appear to be controversial and a radial flow remains a good approximation when averages are made over a solar rotation (Mariani and Neubauer 1990). The initial positions of the planets at the epoch of dust ejection are derived from the ephemerides JPL DE200.

#### 4. Results

The dynamical behaviour of comet–derived dust grains is strongly influenced by gravitational perturbations of the plan-

ets, in particular Jupiter, by radiation/solar–wind pressures and by Poynting–Robertson drag forces. The gravitational encounters with the planets scatter the particles randomly in the orbital phase space driving them in a chaotic route while the retarding forces (P–R drag), which act as major perturbative forces on grains with radii between 1 and  $100 \mu\text{m}$ , cause a monotonic decrease of semimajor axis and eccentricity of the particle orbit with a consequent fall–in toward the Sun. Under these effects the dust particles lose their initial orbital elements on a short timescale and spread around the comet orbit.

We have performed a large number of model computations of the dynamical evolution of dust particles ejected by two SPC with the following goals:

- 1) to predict the spatial distribution of the dust after a long timespan from emission and the contribution to the zodiacal cloud;
- 2) to evaluate the relevance of the P–R drag compared with the planetary gravitational perturbations;
- 3) to state the significance of using a detailed model to compute the ejection velocities of the grains in predicting the spatial distribution of the dust at subsequent times;
- 4) to estimate the fraction of grains lost from the Solar System on hyperbolic orbits.

The two comets under study (P/SW1 and P/GS) have been selected since they have significantly different orbital parameters. Comet SW1 has a moderate eccentricity (0.0447) and the perihelion at about 5.7 AU between the orbits of Jupiter and Saturn, so its orbital evolution is strongly influenced by the gravitational perturbations of the two planets. The perihelion of comet P/GS is located around 1.1 AU and the orbit has a high eccentricity (0.665), so the comet is perturbed by Jupiter only close to the aphelion. A different balancing between P–R drag and gravitational scattering has to be expected for dust particles released by the two comets. Under this point of view, the choice of these comets allows us to cover a wide range of dynamical behaviours distinctive of cometary dust particles.

In Fig. 1 we visualize the spatial distribution of dust grains of two different sizes ( $10 \mu\text{m}$  – filled triangles,  $100 \mu\text{m}$  – empty squares) obtained numerically integrating the orbits of  $\sim 700$  particles for a timespan of  $5 \cdot 10^3$  years. The initial orbital elements of the grains have been computed with the Fulle’s model assuming an isotropical emission geometry. The positions of the particles are projected on the x–y plane, i.e. the ecliptic plane of J2000. The spreading of the grains around the comet orbit is due to repeated encounters with both Jupiter and, to less extent, Saturn. The contribution of Saturn can be inferred from Fig. 2a where the orbital elements of the grains are plotted together with the Tisserand invariant of the comet at different evolutionary times ( $1 \cdot 10^3$ ,  $5 \cdot 10^3$  and  $2 \cdot 10^4$  years). Jupiter is the main perturbing planet and in fact initially the particles shift along the invariant line, but also Saturn influences the orbits of the grains scattering the particles around the invariant. The amount of spreading is increased significantly after  $2 \cdot 10^4$  while about 7% of the initial grains have been ejected out of the Solar System. This percentage increases to 17% after  $5 \cdot 10^4$ . We conclude that only 1% of dust grains emitted by P/SW1 reaches the Sun

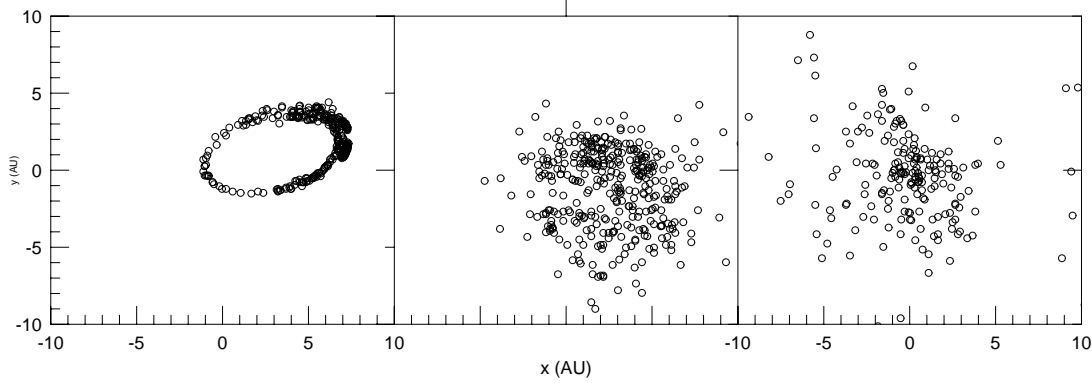


**Fig. 4.** Spatial distribution at different evolutionary ( $10^3$ ,  $5 \cdot 10^3$  and  $2 \cdot 10^4$  years) of  $20 \mu\text{m}$  dust grains emitted by the P/GS at 1992 perihelion passage.

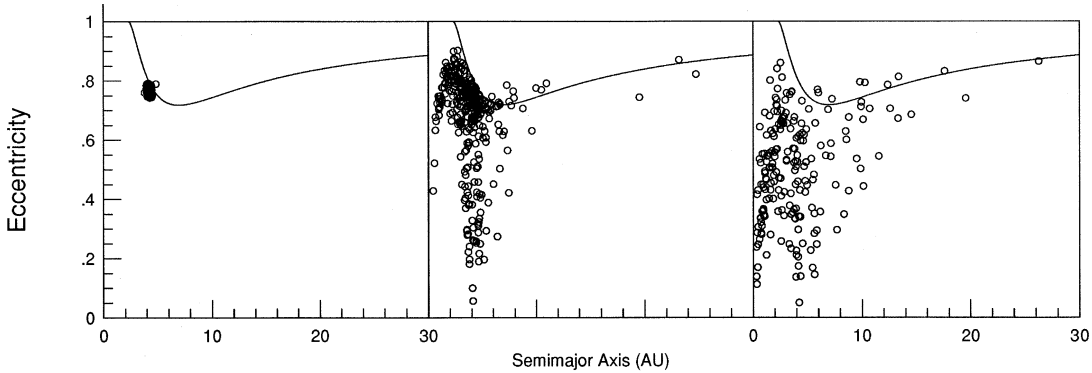


**Fig. 5.** Orbital distributions at different times ( $10^3$ ,  $5 \cdot 10^3$  and  $2 \cdot 10^4$  years) of  $20 \mu\text{m}$  grains emitted by P/GS.

distance of 1 AU and contributes to the inner zodiacal cloud. About 80% of the grains are spread in a wide region outside 4 AU and are slowly ejected from the Solar System if they are not destroyed on a shorter timescale by collisions. In Fig. 2b the orbital evolution of grains from P/SW1 is computed including in the P–R drag the non–radial term. In this case the ratio between the corpuscular and radiation drag forces is about 1 and, as a consequence, a faster orbital decay is expected. Comparing Fig. 2a with Fig. 2b (only 300 particles have been integrated in the simulation of Fig. 2b against the 800 in Fig. 2a), we see that when the drag is stronger (Fig. 2b) few particles detach from the Tisserand invariant line, and so from the Jupiter gravitational influence, and drift toward the Sun under P–R drag. However the percentage of grains which escape from the Jupiter influence and evolve only under P–R drag is very small and we can assume that the P/SW1 cometary grains are not sensitive to the drag model.

In order to verify that the spatial evolution of the grains is not conditioned by a) the particular geometry of ejection from the cometary nucleus b) by the position of the comet in its orbit at the moment of emission, we have performed two additional numerical simulations. In the first simulation we have assumed a conical ejection geometry for the grains: the opening of the cone is  $90^\circ$  (half opening  $45^\circ$ ) and the symmetry axis always pointing toward the Sun. In the second simulation we integrate

the trajectories of grains ejected at different locations along the comet orbit ( $t = -782.6, -640.1, -499.1, -359.6, -220.9, -82.7$  days before perihelion passage). In Fig. 3 we compare the distribution of the perihelia at  $t = 2 \cdot 10^4$  years for these different sets of particles. No significant differences can be detected among the three histograms.

This last result confirms that the evolution of dust grains released by P/SW1 is dominated by chaotic phenomena associated with repeated close approaches both to Jupiter and Saturn. The grain orbits are characterized by random impulsive changes of the orbital elements in correspondence to each close encounter and, as a consequence, they lose memory of their initial orbital parameters on a short timescale ( $\sim 10^3$  years). Due to the high frequency of close encounters, the P–R drag is not a relevant perturbing force for dust particles since in most of the cases it does not have enough time to accumulate relevant orbital changes between two subsequent encounters. Only few particles, in particular the smaller ones, avoid close encounters with both planets for an interval of time sufficiently long to be driven by P–R drag toward the Sun.

Different is the behaviour of dust grains released by comet P/GS. We used again the Fulle’s model to generate starting conditions for dust grain trajectories, assuming a spherical distribution of the ejection velocities. We had also to consider a single location of the comets in its orbit due to the lack of observative

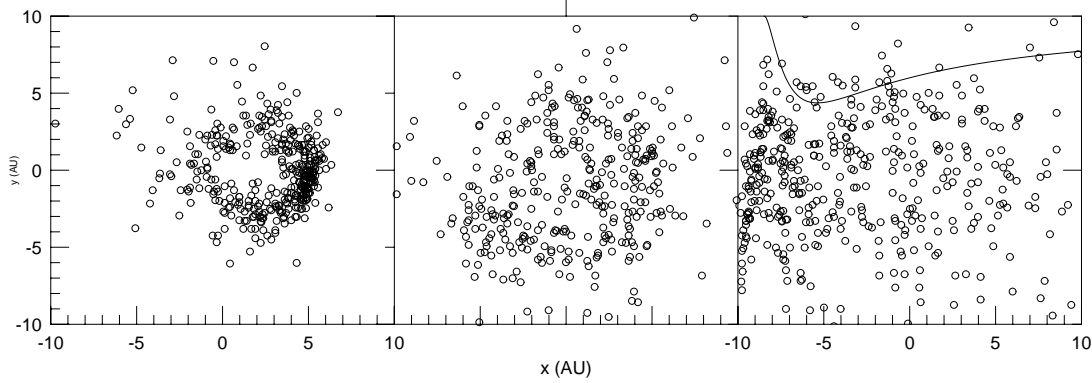


**Fig. 6.** Same as Fig. 4 for  $200\mu\text{m}$  size grains

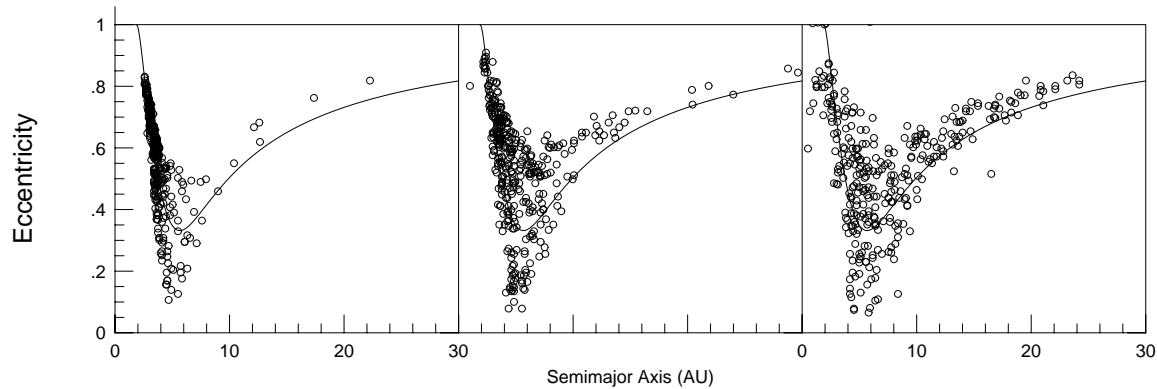


**Fig. 7a.** Same as Fig. 5 for  $200\mu\text{m}$  size grains

data to be used in the Fulle's model.  $20\mu\text{m}$  size particles are strongly influenced by P–R drag during the perihelion passage located very close to the Sun and they evolve quite rapidly toward the Sun on a timescale of the order of few thousand years. The spatial distributions displayed in Fig. 4 at  $t=1\ 10^3$ ,  $t=5\ 10^3$  and  $t=2\ 10^4$  years, respectively, show a progressive shrinking of the grain cloud toward the Sun. In particular after  $t=2\ 10^4$  years about 47% of the grains have reached a perihelion distance lower than 0.3 AU from the Sun and have to be considered as completely vaporized. The gravitational perturbations by Jupiter are not very effective compared to the P–R drag as visualized in Fig. 5. Only few grains follow the invariant line while most of the grains exhibit a progressive damping of the eccentricity and decrease of the semimajor axis. When we include the non-radial term in the drag force, the drift of grains toward the Sun is faster and after  $t=1.2\ 10^4$  years all the particles in our simulation are fallen into the Sun.

The corresponding spatial and orbital distributions for  $200\mu\text{m}$  size particles are shown in Figs. 6–7a,b. A higher correlation is observed in Fig. 7a,b (in the simulation of Fig. 7b the non-radial term in the drag force has been included) with the invariant line due to the decreased strength of the non-gravitational forces. Jupiter is very effective in scattering the particles when they are at the aphelion and also in simulation b, when the drag force is stronger, the orbital evolution of P/GS

grains is dominated by the gravity of the planet. The spatial distribution, compared to the one for  $20\mu\text{m}$  size particles, is more diffuse and less concentrated around the Sun. Only 6% of the grains fall into the Sun after  $2\ 10^4$  years. The initial eccentricity damping trend is reversed by Jupiter perturbations which push particles back to higher eccentricities and larger semimajor axes following the invariant line. The different behavior of 20 and  $200\mu\text{m}$  particles is evidenced in Fig. 8 that shows the distributions of their perihelia. The histogram for  $20\mu\text{m}$  particles has a maximum around 0.5 AU induced by the high P–R decay rate while the  $200\mu\text{m}$  histogram is uniformly distributed with a peak around 4.5 AU produced by the Jupiter perturbations. The results of these simulations suggest that there is a slow change in the behavior of dust particles emitted by P/GS depending on their size. Particles smaller than  $20\mu\text{m}$  drift toward the Sun on short timescales ( $\sim 2\ 10^4$  years or less, depending on their size) without being affected by Jupiter. As the size of the dust particles increase, a larger percentage of them are scattered along the Tisserand invariant line by close encounters with Jupiter and contribute to the zodiacal dust cloud for a longer time (on highly eccentric orbits). Their final fate is ejection from the Solar System on a timescale of the order of  $\sim 2\ 10^5$  years, having an orbital evolution similar to that of short period comets.

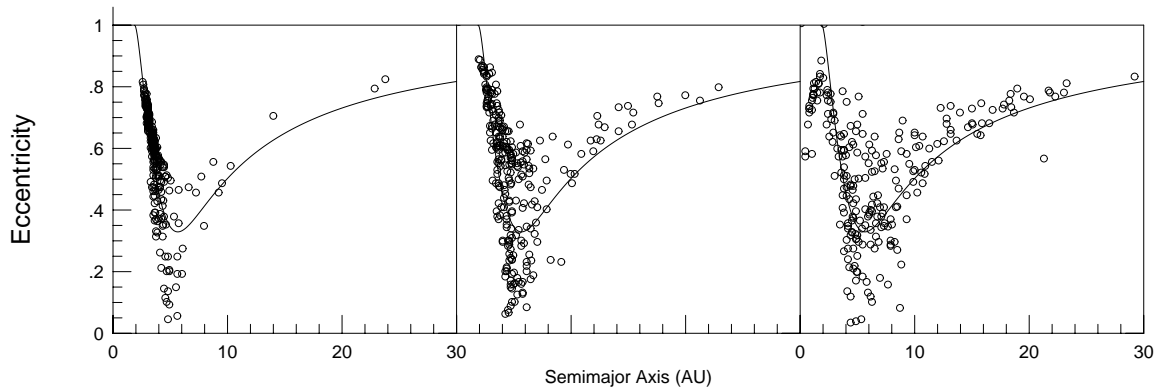


**Fig. 7b.** Same as Fig. 7a but including in the drag force the non-radial term

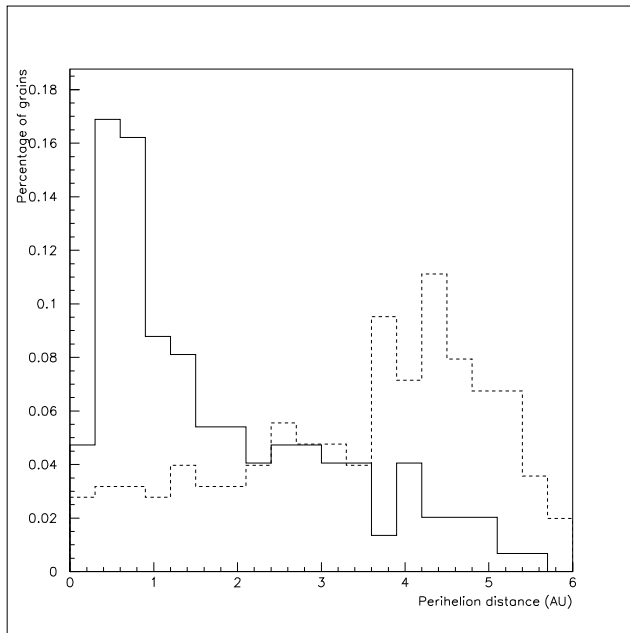


**Fig. 8.** Perihelia distributions at  $t=2 \cdot 10^4$  years for  $20 \mu\text{m}$  particles (continuous line) and  $200 \mu\text{m}$  particles (dashed line)

## 5. Discussion

We have performed an accurate modelling of dust trajectories starting from cometary emission (Fulle's model) and then following the subsequent orbital evolution integrating the Newton equations. Among SPC we have selected P/GS and P/SW1 which represent two significantly different objects from a dynamical point of view. The orbital evolution of dust particles emitted by these two comets is then well representative of the possible behaviours of cometary dust grains because of the different balancing between P-R drag and Jupiter perturbations.

For P/SW1 grains, Jupiter perturbations force the particles in highly chaotic routes and, as a consequence, memory of the initial conditions are lost on a short timescale as shown by comparing the perihelia distributions of the grain clouds characterized by different ejection configurations. Because P-R drag

is not a leading force, the size of the particles is not relevant for the dynamical behaviour. Very few particles produced by P/SW1 reach the inner region of the Solar System and the sink mechanism is not vaporization by the Sun, but ejection from the Solar System or collisions.

For P/GS grains again the Tisserand invariant represents a useful criterion for estimating the relevance of the P-R drag in perturbing the grain orbits.  $20 \mu\text{m}$  particles are dominated by P-R drag and rapidly fall into the Sun. Most of the  $200 \mu\text{m}$  particles follow the Tisserand invariant as they are kept far from the Sun having a longer lifetime.

We conclude that Jupiter perturbations oppose to the P-R drag forces and reduce significantly the contribution of SPC to the inner zodiacal dust cloud in two ways:

- 1) preventing particles to spiral towards the Sun
- 2) increasing the average eccentricity and reducing consequently the mean density of particles in the inner regions.

This implies that the contribution to the zodiacal dust mass supplied from SPC estimated simply adding up the values of the dust productions rates could be overweighted.

A further useful use of the Tisserand invariant could consist in distinguishing the parent sources of meteoroids collected with near Earth space platforms. If accurate measurements of the velocity vectors are performed, the orbital elements of the grains (in particular larger grains) could be associated, through the invariant curve, to the parent cometary source.

*Acknowledgements.* We are grateful to the reviewer B.A.S. Gustafson for many valuable comments and discussions. This work was supported in part by the Italian Space Agency (ASI).

## References

- Brownlee D.E., Kissel J., 1990, Comet Halley: investigations, results, interpretations, edited by John Mason, vol.2, 89
- Cremonese G., Fulle M., 1989, *Icarus* 80, 267
- Crifo J.F. 1987, in Rolfe E.J., Battrick B. (eds.), *Diversity and Similarity of Comets* ESA SP-278, Paris, 399
- Crifo J.F. 1991, in Newburn R.L.Jr., Neugebauer M., Rahe J. (eds.), *Comets in the Post-Halley Era*, Kluwer, Dordrecht, 937

- Everhart E., 1985. In: Carusi A., Valsecchi G.B. (eds.) Proc. IAU Coll. 83, Dynamics of comets: their origin and evolution. Reidel, Dordrecht, p.185
- Finson M.L., Probst R.F. 1968, ApJ 154, 327
- Fulle M. 1987, A&A 171, 327
- Fulle M. 1989, A&A 217, 283
- Fulle M. 1992, Nature 359, 42
- Fulle M., Sedmak G., 1988, Icarus 74, 383
- Fulle M., Cremonese G., Jockers K., Rauer H., 1992, A&A 253, 615
- Fulle M., Mennella V., Rotundi A., Colangeli L., Bussoletti E., Pasian F., 1993, A&A 276, 582
- Gombosi T.I., 1986 in Battrick B. et al. (eds.), Exploration of Halley's Comet (Vol. 3), ESA SP-250, Paris, 167
- Gustafson B.A.S., 1994, Ann. Rev. Earth Planet. Sci., 22,553
- Grün E., Zook H.A., Fechtig H., Giese R.H., 1985, Icarus 62, 244
- Jewitt D., 1990, ApJ, 351, 277
- Kimura H., Liu C.P., 1977, Chin. Astr. 1, 235
- Marzari F., Vanzani V., 1994a, Planet. Space. Sci. 42, 101
- Marzari F., Vanzani V., 1994b, A&A 283, 275
- Mukai T., 1989, Cometary dust and interplanetary particles. In: Bonetti A., Greenberg J.M., Aiello S. (eds.) Proc. Intern. Sch. Phys. E. Fermi Course CI, Evolution of interstellar dust and related topics. North-Holland, Amsterdam, p.397
- Mukai T., Yamamoto T., 1982, A&A 107, 97
- McDonnell J.A.M., et al. 1992, Nature 362, 732
- Richter K. Keller H.U., 1987 A&A 171, 317
- Senay M.C., Jewitt D.C., 1994, Nature 371, 229
- Wallis M.K. 1982, in Wilkening L.L. (ed.), Comets, Univ. of Arizona Press, 357